(Received 7 October 2024, Accepted 26 November 2024, Scheduled 31 December 2024)

A Novel Miniature Inverted `V' Slot Reconfigurable Patch Antenna for X-Band Applications

Bathula Ashok Kumar[1, *], Vijaya Chandra Kavuri[2], Gudla Ramalakshmi[3], and Moturi Satyanarayana[4]

[1]Department of ECE, Sri Vasavi Engineering College (A), Tadepalligudem, A.P, India
[2]Department of Electronics and Communications Engineering, PACE IT & S, Ongole, A.P, India
[3]ECE Department, Mahaveer Institute of Science and Technology, Bandlaguda, Hyderabad, T.S, India
[4]Department of ECE, MVGR College of Engineering, Vizianagaram, A.P, India

ABSTRACT: A reconfigurable patch antenna for X-band applications offers frequency agility and adaptability for systems operating within the 8–12 GHz range. This design allows dynamic tuning of the antenna's operating frequency, making it ideal for radar, satellite communications, and military applications. By incorporating reconfigurable elements, such as switches or tunable materials, the antenna can adjust to varying operational requirements, improving performance and flexibility in compact systems where space and efficiency are crucial. A reconfigurable patch antenna for X-band applications faces several challenges. Incorporating reconfigurable elements, such as switches or tunable materials, can increase the design's complexity and reduce reliability, especially in high-frequency X-band operations. Miniaturization may result in performance trade-offs, potentially affecting the antenna's gain, bandwidth, and radiation efficiency. Additionally, ensuring stable and interference-free operation across the reconfigured frequencies can be difficult. The antenna's power-handling capability may also be limited, which is critical for radar and military applications. Finally, thermal stability and environmental resilience are key concerns, as performance can degrade under varying conditions. Hence, this paper proposes a novel miniature inverted V-slot reconfigurable patch antenna. The extended antenna design features a compact radiating patch (10.5 mm × 14 mm) with an inverted 'V' slot and corner modifications (chamfering) to enhance performance. Frequency and polarization reconfiguration are achieved through the enable/disable functionality of PIN diodes placed within the inverted 'V' slot, allowing dynamic adjustments. The defected ground structure, featuring two vertical slots, further aids in enhancing the antenna's operational capabilities. The antenna operates across multiple frequency bands, specifically 9.84–10.46 GHz, 10.66–11.59 GHz, 11.08–11.98 GHz, and 11.61–12.11 GHz, making it suitable for X-band applications. Additionally, the proposed antenna supports right-hand circular polarization (RHCP), left-hand circular polarization (LHCP), and linear polarization (LP), offering versatile propagation modes. Both practical and simulated results demonstrate good impedance matching across different polarization states. This design is highly suitable for satellite communication and other X-band applications due to its reconfigurable and flexible performance.

1. INTRODUCTION

Reconfigurable patch antennas for X-band applications have gained significant attention due to their ability to adapt to varying operational requirements in systems like radar, satellite communications, and military devices [1–4].

These antennas offer the advantage of frequency and polarization reconfiguration, allowing dynamic tuning of their performance within the 8–12 GHz X-band spectrum [5]. By integrating elements like PIN diodes or tunable materials, reconfigurable patch antennas can modify their radiation characteristics in real-time, optimizing efficiency in compact, high-performance systems [6–9]. This adaptability not only enhances versatility but also reduces the need for multiple fixed-frequency antennas, making reconfigurable designs an ideal solution for modern communication and sensing technologies [10]. The design of reconfigurable patch antennas typically involves innovative geometries and materials that facilitate effective frequency agility and polarization manipulation [11]. For instance, incorporating features like inverted slots or defected ground structures can significantly improve the antenna's performance metrics, such as bandwidth, gain, and efficiency. The ability to operate in multiple polarization states — right-hand circular polarization (RHCP), left-hand circular polarization (LHCP), and linear polarization (LP) — further enhances their applicability in diverse scenarios, allowing seamless integration into existing communication systems [12–15].

Moreover, the miniaturization of these antennas without compromising performance is crucial for space-constrained applications, particularly in satellite and mobile communications [16]. As the demand for flexible and high-performance antennas continues to grow, ongoing research and development in reconfigurable patch antennas are vital for advancing next-generation wireless technologies.

The high-efficiency wireless communication service requires the reconfigurability in radiation characteristics such as pattern, polarization, and frequency or amalgamation of these characteristics, on board [17]. The fast development of cognitive radio field and the tendency toward miniaturization and multi-service in wireless systems created a substantial

* Corresponding author: B. Ashok Kumar (bashokkumar2021@gmail.com).

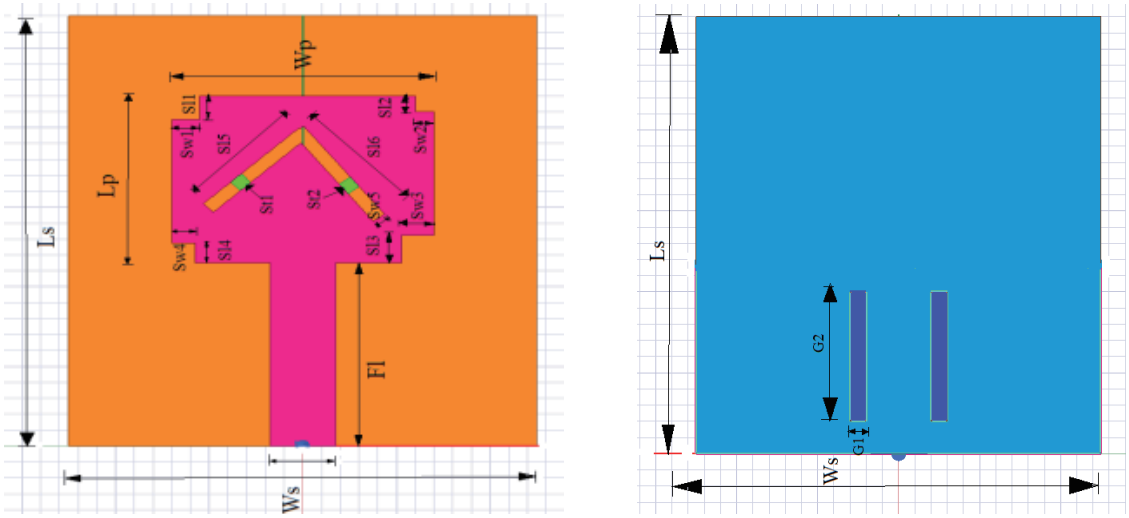

FIGURE 1. Geometry of a novel miniature frequency and polarization diversity patch.

need to increase the performance of antennas and to design higher flexible antennas capable of accommodating their operating frequencies with the situation concern [18]. Hence, an enormous amount of research has been accomplished to design antennas as well as frequency cleverness characteristics [19]. The main aim for the design of such antennas is the capability to cover various wireless communication applications and the better utilization of the frequency spectrum.

X-band applications encompass a wide range of technologies primarily operating within the 8 to 12 GHz frequency range, making them integral to various communication and radar systems [20]. This frequency band is widely utilized in satellite communications, enabling reliable data transmission for both commercial and military purposes. In radar systems, X-band frequencies are favored for their ability to provide high-resolution imagery and accurate target detection, making them ideal for weather monitoring, air traffic control and defense surveillance applications [21]. Additionally, X-band frequencies are increasingly employed in wireless communication systems, including 5G networks, where they support high data rates and improved connectivity. The versatility of X-band applications is further enhanced by advancements in antenna technology, such as reconfigurable patch antennas, which allow for dynamic frequency and polarization adjustments to meet diverse operational needs [22]. As demand for efficient and robust communication solutions grows, X-band applications are positioned at the forefront of technological innovation, playing a critical role in both civilian and military domains. To attain reconfigurability, the antenna needs some radio frequency electronically operated switching devices like micro-electromechanical system (MEMS) switches, field effective transistor (FET)'s and PIN diodes. The switch selection depends on the type of application, switching speed, and power handling capacity. To improve the communication system capacity, reconfigurable antennas are preferable [23]. Further, many reconfigurable antennas switching from linear to circular polarization have been addressed in past literature.

In this proposed design radiating patch four corners are chamfering with different lengths and widths for achieving frequency reconfiguration and inverted 'V' model slot on the center of the antenna, which is used for achieving polarization diversity. To change the polarization, 2 PIN diode switches are embedded into the inverted 'V' slot. DGS (Defected ground structure) technique is used in the proposed design. This technique does not require any supplementary volume, cost, substance, or material and has been favorable in minimizing crosspolarization (XP). Simulation work is carried out using HFSS17. Moreover, simulation results were endorsed by correlating the measured and simulated results which display an excellent compliance between them.

2. RECOMMENDED DESIGN WITH FREQUENCY AND POLARIZATION RECONFIGURABLE CAPABILITIES

The design of the recommended rectangular microstrip antenna is shown in Fig. 1. The rectangle patch's length $L_p = 10.5$ mm, width $W_p = 14$ mm, and height of the substrate is $h = 1.6$ mm. The patch is etched on a sheet of FR-4 with a dielectric constant of $\varepsilon_r = 4.4$. Four corners of the radiating patch are chamfering with the dimensions of $1.5 \times 1.5\,\text{mm}^2$, $1 \times 1\,\text{mm}^2$, $1.75 \times 1.75\,\text{mm}^2$, and $1.25 \times 1.25\,\text{mm}^2$, respectively. An inverted 'V' shape slot is on the radiating patch with dimensions of $7 \times 0.75\,\text{mm}^2$. A $50\,\Omega$ microstrip feed line with the dimensions of $11.5 \times 3.5\,\text{mm}^2$ is used in this design. Defected ground structure (DGS) with the dimensions of $1 \times 8\,\text{mm}^2$ is used to minimize the cross-polarization. The proposed design geometry dimensions are shown in Table 1.

1. **Impedance Matching**: Slots in the ground plane contribute to fine-tuning the impedance of the antenna. Excess solder may fill or cover the slots, altering the current distribution and potentially disrupting the resonance conditions. This can lead to impedance mismatch, increasing reflection losses and potentially impacting the antenna's VSWR (Voltage Standing Wave Ratio). As a result, you

TABLE 1. Proposed antenna geometry dimensions.

Parameter	L_s	W_s	L_p	F_l	$Sl1$	$Sl2$	$Sl3$
Dimensions	27	25	10.5	11.5	1.5	1	1.75
Parameter	$Sl4$	$Sl5$	$Sl6$	$Sw1$	$Sw2$	$Sw3$	$Sw4$
Dimensions	1.25	7	7	1.5	1	1.75	1.25
Parameter	$Sw5$	$St1$	$St2$	$G1$	$G2$	$Lg1$	$Lg2$
Dimensions	0.75	$0.75*0.75$	$0.75*0.75$	1	8	25	11.5

might observe degraded matching, especially at target frequencies, which could reduce the operational bandwidth.

2. **Radiation Pattern**: The ground plane slots help control the radiation pattern by shaping the current flow. When these slots are obstructed, the current distribution on the ground plane might be different from that intended, resulting in altered radiation patterns. This could lead to unintended side lobes, shifts in the main beam direction, or a more irregular radiation pattern, potentially reducing the antenna's directivity.

3. **Antenna Efficiency**: Excessive solder might introduce additional losses, which can absorb part of the radiated power, reducing the overall efficiency of the antenna. Furthermore, if the solder is unevenly applied, it could lead to imbalances that influence radiation efficiency, causing more power to be dissipated in the solder instead of being radiated.

In testing, these flaws may cause increased return loss, altered resonance peaks, and lower gain values. The proposed antenna design features a novel miniature frequency and polarization diversity patch, as illustrated in the provided geometry and fabrication images. The antenna geometry is characterized by specific dimensions that enhance its performance, including a total length (Ls) of 27 mm and a width (Ws) of 25 mm. Key parameters include a patch length (Lp) of 10.5 mm and various slot dimensions such as $Sl1$, $Sl2$, and $Sl3$ measuring 1.5 mm, 1 mm, and 1.75 mm, respectively. Additionally, the design incorporates a feed line length (Fl) of 11.5 mm, contributing to the antenna's impedance matching and overall efficiency.

The fabrication of the antenna is depicted in the images, showcasing both the top and bottom views. The top view reveals the intricate slot design and layout, while the bottom view highlights the connection to the feeding mechanism. These dimensions and the unique geometry are critical for achieving the desired frequency reconfiguration and polarization diversity, making this antenna suitable for applications in X-band communication systems. The compact and innovative design aims to meet the increasing demand for versatile and high-performance antennas in modern telecommunications.

The resonant frequency of a rectangular patch antenna can be estimated using the following formula:

$$f_r = \frac{c}{2L_{eff}\sqrt{\varepsilon_r}} \tag{1}$$

In Eq. (1) f_r is stated as resonant frequency; c is the defined speed of light in vacuum (approximately 3×10^8 m/s); L_{eff} is defined as effective length of the patch; and ε_r is stated as the relative permittivity of the substrate material. The effective length can be approximated as:

$$L_{eff} = L_p + 2\Delta L$$

where ΔL is the length extension due to the fringing fields, calculated using Eq. (2)

$$\Delta L \approx \frac{0.412h\,(\varepsilon_r+0.3)\,(W_p+0.264h)}{(\varepsilon_r-0.258)\,(W_p+0.8h)} \tag{2}$$

In Eq. (2), h is stated as the height of the dielectric substrate and W_p defined as the width of the patch. The input impedance Z_{in} of the patch antenna is stated as in Eq. (3)

$$Z_{in} = \frac{Z_0}{1+j\left(\frac{L-L_P}{W_p}\right)} \tag{3}$$

In Eq. (3), Z_0 is stated as the characteristic impedance of the feed line (usually 50 Ohms) and L defined as length of the feed line. To change the frequency and polarization states of the proposed antenna, 2 PIN diode switches are infused near the brink of the slits with diodes $St1$ and $St2$. The recommended antenna has four frequency reconfigurable and two main polarization states (LP&CP), and the selection of the frequency band and polarization is ON/OFF condition of the PIN diode switches. Fig. 2 shows top and bottom views of the fabricated antenna. The polarization diversity in antennas can be described using the polarization states. For circular polarization (CP), the axial ratio (AR) is stated as follows

$$\mathrm{AR} = \frac{E_{\max}}{E_{\min}}$$

where $E_{\max}$ and $E_{\min}$ are the maximum and minimum electric field components. The antenna can be designed to switch among RHCP, LHCP, and linear polarizations by adjusting the feeding mechanism or incorporating PIN diodes in specific slots. The design is verified through simulations using software tools like HFSS or CST Microwave Studio, where parameters like return loss (S_{11}), gain, and radiation patterns are analyzed with **Return Loss** calculated using Eq. (4)

$$S_{11} = 20\log\left(\frac{Z_{in}-Z_0}{Z_{in}+Z_0}\right) \tag{4}$$

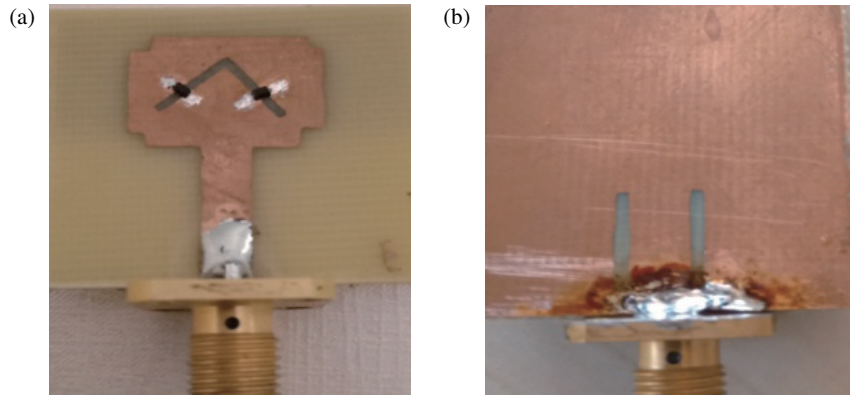

FIGURE 2. Fabricated antenna. (a) Top view, (b) Bottom view.

A return loss less than -10 dB typically indicates good impedance matching. Through the consideration of the above stated Eqs. (1)–(4), the optimization features are computed with trial and error method.

2.1. Frequency Reconfiguration

To achieve frequency reconfiguration, microstrip patch four corners are chamfering with four different dimensions, and inverted 'V' shaped slot is introduced in the middle of the patch. Two switches (PIN diodes) are introduced in the slots. Bias voltage is applied to the PIN diodes to change the switching state of the diode from ON to OFF and vice versa. In simulation, PIN diodes are replaced by using lumped RLC network. The ON diode low impedance is 4.7 Ω, and OFF diode high impedance is a parallel combination of 40 kΩ resistance and 0.033 pf capacitance. SMP1320-079LF PIN diodes are used in the recommended design. In the proposed design frequency, reconfiguration is achieved by changing the electrical path length of the patch.

To optimize the performance of the patch antenna, the four corners of the patch are modified or "chamfered" with different dimensions. This alteration creates a unique shape that enhances the antenna's radiative properties and influences its resonant frequencies.

In addition to this modification, an inverted 'V' shaped slot is introduced in the center of the patch. This slot plays a critical role in altering the electrical characteristics of the patch, specifically its resonant frequency. The shape and placement of the slot allow for the manipulation of the current distribution across the patch, which is essential for achieving the desired frequency reconfiguration.

To enable frequency reconfiguration, two switches in the form of PIN diodes are strategically placed within the inverted 'V' slot. The operation of these diodes is controlled by applying a bias voltage, which changes their state from ON to OFF and vice versa:

- **ON State**: When the diode is in the ON state, it presents a low impedance of approximately 4.7 Ω, allowing current to flow freely through the diode. This effectively changes the current distribution in the antenna and alters the resonant frequency.
- **OFF State**: Conversely, when the diode is in the OFF state, it presents a high impedance. In this case, a parallel combination of a 40 kΩ resistor and a 0.033 pF capacitor is used to simulate the high impedance condition. This change in impedance affects how the antenna radiates energy, thus modifying its operational frequency.

In the simulation phase, the actual PIN diodes are replaced by a lumped RLC network to represent their behavior without using the physical diodes. This simplification allows for an easier analysis of the antenna's performance under different bias conditions.

The lumped RLC network incorporates:

- **Resistance (R)**: Represents the ON state of the diode (4.7 Ω).
- **Inductance (L)**: Can be introduced to represent the inductive effects in the circuit.
- **Capacitance (C)**: Simulates the OFF state with a combination of a high-value resistor (40 kΩ) and a small capacitor (0.033 pF), effectively modeling the diodes' impact on the overall impedance.

The design leverages the structural modifications of the microstrip patch, along with the strategic implementation of PIN diodes to enable frequency reconfiguration. By controlling the states of the diodes, the antenna can adapt its resonant characteristics effectively, enhancing its versatility for various applications. This approach not only optimizes performance but also demonstrates an innovative solution to meet the increasing demands for reconfigurable antennas in modern telecommunications.

2.2. Polarization Reconfiguration

When the two diode switches are in ON state or OFF state, the antenna radiates linearly polarized waves. The antenna is physically and electrically symmetric in shape. In these two states, antenna is excited in TM_{11} mode. The two diode switches are in

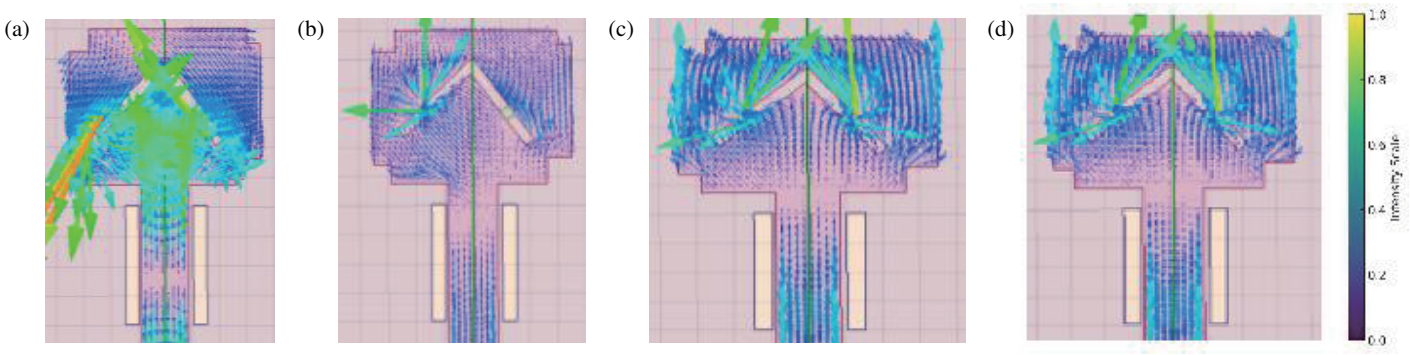

FIGURE 3. The current flow on the surface of proposed antenna at the resonant frequencies. (a) Switches St1-OFF & St2-OFF (LP at 10.2 GHz). (b) Switches St1-ON & St2-OFF (LHCP at 11.06 GHz). (c) Switches St1-OFF & St2-ON (RHCP at 11.62 GHz). (d) Switches St1-ON & St2-ON (LP at 11.88 GHz).

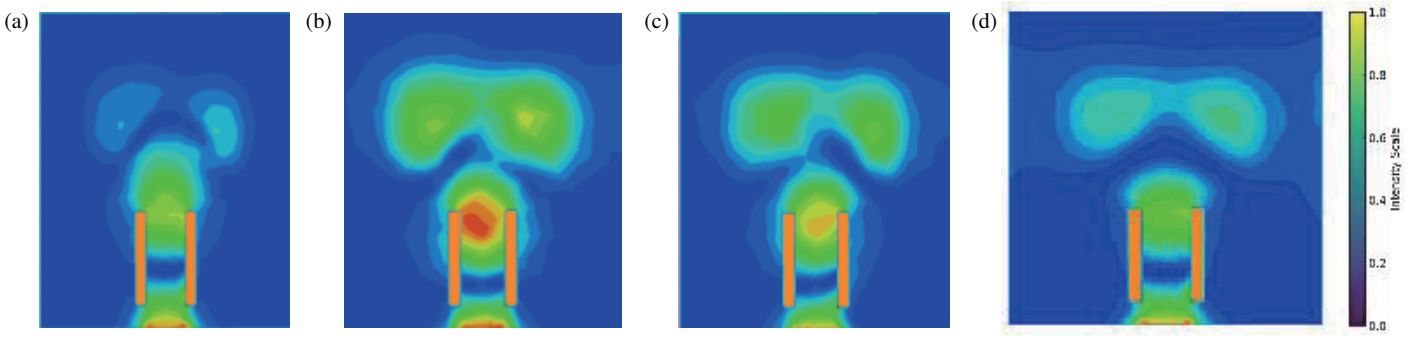

FIGURE 4. The current density on the surface of ground for four switching states. (a) Switches St1-OFF & St2-OFF. (b) Switches St1-ON & St2-OFF. (c) Switches St1-OFF & St2-ON. (d) Switches St1-ON & St2-ON.

ON state, and they behave as a short circuit. So the inverted 'V' shape slot is moderately changed, leading only to a frequency shift without changing the radiation pattern. Two diodes in an OFF state form an open circuit due to their high-impedance paths. In this switching state, objectively and electrically commensurable shape of the patch antenna is presented. In TM_{11} mode, the electric field has one half-wave variation along both axes of the antenna. This symmetrical field distribution leads to a linearly polarized radiation pattern, as the currents on the antenna surface are balanced in both directions. This mode generally provides a broadside radiation pattern, which is often desirable for applications needing maximum radiation perpendicular to the antenna's plane. In this mode, there would be one half-wavelength variation in one direction and no variation in the orthogonal direction. This would create an asymmetric current distribution, potentially leading to different polarization characteristics and a nonuniform radiation pattern that does not match the desired linear polarization. Similarly, the TM_{10} mode would have one half-wavelength variation in one axis and zero in the other. This would not result in a balanced current distribution necessary for linear polarization, and it would typically produce a pattern with nulls along certain directions.

For the circular polarization, one of the diodes should be in ON state, and the other should be in OFF state. The surface current distributions for the four states are shown in Fig. 3.

The current on the surface of an antenna is clockwise for LHCP with the diode switches St1-ON and St2-OFF, and for state St1-OFF and St2-ON, the surface current rotates anticlockwise for RHCP. The balanced shape of these switching states noticed in these images is due to uniformity in the antennas configuration. The aim of the DGS is to reduce the cross polarization generating from rectangular modes and the specious radiations from the feed line simultaneously. The current density on the surface of ground for the four switching states of PIN diodes is shown in Fig. 4.

The image depicts the current flow on the surface of the proposed antenna at a resonant frequency of 10.2 GHz, specifically when both switches St1 and St2 are in the OFF state, indicating linear polarization (LP) operation. This visualization illustrates how electric current propagates across the antenna's surface, showcasing the distribution patterns formed under these conditions. With both switches OFF, the configuration alters the current path, which is crucial for optimizing the antenna's performance. The directed flow of current suggests effective propagation of electromagnetic waves, contributing to good impedance matching and radiation efficiency. The vector field plots are related to an electromagnetic or antenna system. The blue arrows depict the direction and intensity of the field, while green arrows highlight key points of field behavior or transitions. The geometrical structure in pink may represent an antenna or a waveguide. The text refers to different

TABLE 2. Comparison of simulated and measured results.

Switch state		S_{11} [dB]		−10 dB BW [%]		Polarization	Gain [dBi]	Axial ratio [dB]
St1	St2	Simulation	Measurement	Simulation	Measurement			
0	0	14.7	14.1	6.07	6	LP	2.4	N/A
0	1	18.57	16.21	8.4	8.1	LHCP	4.1	1
1	0	44.26	34.6	7.74	7.8	RHCP	4.7	1.2
1	1	21.52	18.5	4.2	4.4	LP	4.5	N/A

switch settings (St1 and St2) that control the polarization of the waves. Specifically, when switch St1 is ON and St2 OFF, the system generates Left-Hand Circular Polarization (LHCP) at a frequency of 11.06 GHz. When St1 is OFF and St2 ON, it produces Right-Hand Circular Polarization (RHCP) at 11.62 GHz. Additionally, when both switches are ON, the system produces Linear Polarization (LP) at 11.88 GHz. These images likely demonstrate how different switch configurations influence the polarization and field patterns at various frequencies, which is typical in the design and analysis of antenna systems.

Figure 4 illustrates the current density on the surface of the ground plane for four distinct switching states of the proposed antenna, providing insights into how different configurations affect current distribution. In panel (a), with switches St1 and St2 both in the OFF state, the current density is concentrated in specific areas, indicating a particular resonant behavior. In panel (b), when St1 is ON and St2 OFF, the current density shifts, demonstrating how enabling St1 alters the current flow and influences the antenna's operational characteristics. Panel (c) shows the scenario where St1 is OFF and St2 ON, revealing another unique distribution of current density, which highlights the interaction between the switches and their impact on the antenna's performance. Finally, in panel (d), both switches are ON, resulting in a different current density pattern that suggests a further modification of the antenna's electromagnetic properties.

3. ANTENNA OUTCOME AND DISCUSSION

This section presents the simulated and measured results like voltage standing wave ratio (VSWR), return loss (RL), radiation pattern, gain, and the axial ratio of the recommended antenna for the four different switching states. The structure of the proposed antenna is altered by changing the switching states of the PIN diodes. The simulated and measured return losses of the proposed antenna are shown in Fig. 5.

The fine points of the antenna design specifications and the results achieved for the 4 different switching states of the recommended antenna design are summarized in Table 2. The proposed antenna operates in four different bands which are 9.84–10.20 GHz, 10.66–11.59 GHz, 11.08–11.98 GHz, and 11.61–12.11 GHz, respectively.

Each band is achieved by switching the state of the diode switches. The bandwidth for the circular polarization is (8.4% for St1-ON & St2-OFF and 7.74% for St1-OFF & St2-ON) larger than the LP (6.07% for St1 & St2-OFF and 4.2% for St1 & St2-ON) because in the case of CP two resonant modes radiate simultaneously, but in LP one resonant mode (TM_{11}) radiates. The steady VSWR of the proposed antenna is shown in Fig. 6. The steady VSWR in four states is observed $\leq$ 2. The design specifications and performance outcomes of the proposed antenna for the four different switching states are succinctly summarized in Table 2. This innovative antenna operates across four distinct frequency bands: 9.84–10.20 GHz, 10.66–11.59 GHz, 11.08–11.98 GHz, and 11.61–12.11 GHz. Each frequency band is selectively accessed by toggling the states of the diode switches integrated into the antenna design. This reconfiguration capability allows for versatile ap-

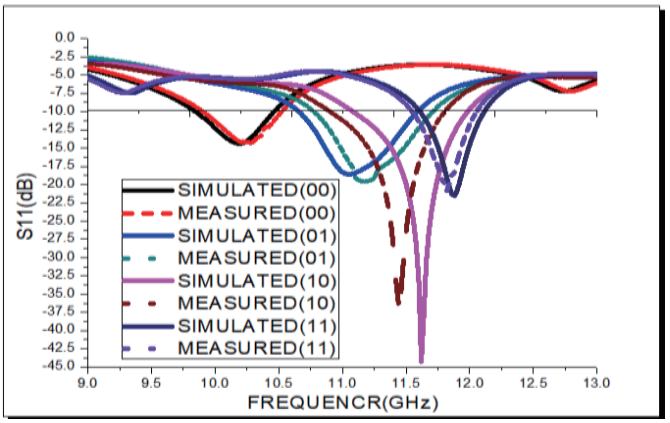

FIGURE 5. Measured and simulated return losses of the proposed design (0-Diode OFF and 1-Diode ON).

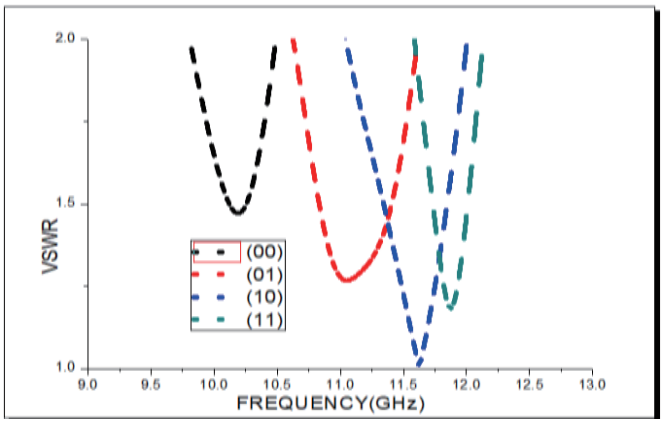

FIGURE 6. Measured VSWR of the recommended antenna (0-diode OFF & 1- diode ON).

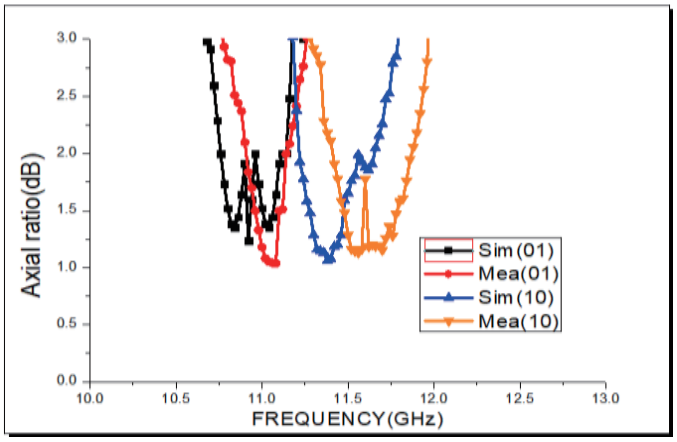

FIGURE 7. Axial ratio plot of the proposed antenna (0-Diode OFF and 1-Diode ON).

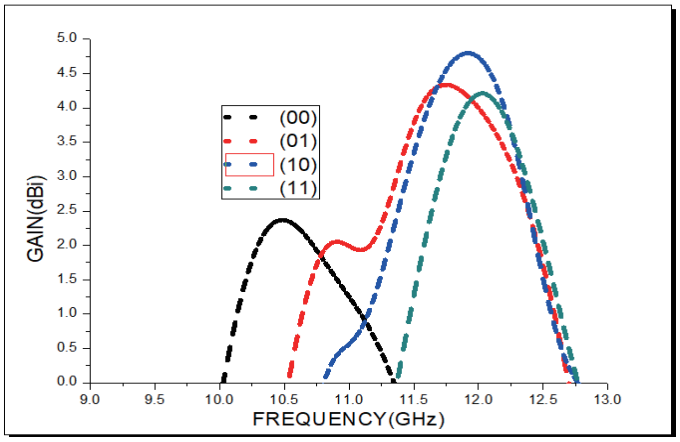

FIGURE 8. Proposed antenna gain vs frequency plot (0-Diode OFF and 1-Diode ON).

plications, making the antenna suitable for various communication systems.

In terms of bandwidth, the antenna demonstrates superior performance in circular polarization (CP) compared to linear polarization (LP). Specifically, the bandwidth for CP is measured at 8.4% when St1 is ON and St2 OFF, and 7.74% when St1 is OFF and St2 ON. In contrast, the LP bandwidths are narrower, recorded at 6.07% for both switches OFF and 4.2% for both switches ON. This disparity in bandwidth can be attributed to the nature of the radiating modes; CP utilizes two resonant modes that operate simultaneously, whereas LP relies solely on one resonant mode (TM_{11}) for its radiation characteristics.

Furthermore, the VSWR for the proposed antenna is consistently maintained at a steady state of less than or equal to 2 across all four switching states, as illustrated in Fig. 6. A VSWR value below 2 indicates efficient impedance matching, essential for optimal antenna performance. This comprehensive performance analysis underscores the effectiveness of the antenna design in achieving desirable operational parameters across multiple frequency bands while accommodating the different switching configurations.

Figure 7 shows the simulated and steadied axial ratios of the proposed antenna for the circular polarization (CP). The value of axial ratio for CP is achieved less than 3 dB. The antenna radiates LHCP for St1 ON and St2 OFF and RHCP for the state of St1 OFF and St2 ON. A good agreement between simulated and steadied data is observed. Fig. 7 presents a detailed comparison of the simulated and steady-state axial ratio for the proposed antenna when operating in circular polarization (CP) mode. The axial ratio, a critical parameter in evaluating the performance of CP antennas, indicates the quality of the polarization being emitted. For effective circular polarization, an axial ratio of less than 3 dB is typically desirable, as it signifies that the radiated waves maintain a close-to-circular characteristic, which is essential for minimizing distortion in signal transmission.

In the context of the proposed antenna design, the axial ratio values consistently remain below the 3 dB threshold, showcasing the antenna's capability to produce high-quality circularly polarized waves. The operational states of the antenna are characterized by distinct polarization types: when switch St1 is activated (ON) while St2 remains deactivated (OFF), the antenna emits left-hand circular polarization (LHCP). Conversely, with St1 deactivated (OFF) and St2 activated (ON), the antenna transitions to radiating right-hand circular polarization (RHCP). This dual functionality allows the antenna to cater to a broader range of applications, including satellite communication and wireless data transmission, where different polarization states may be required based on environmental conditions or specific system requirements.

The results show a strong correlation between the simulated and steady-state data, confirming the accuracy and reliability of the simulation models used in the antenna design process. This agreement indicates that the antenna's performance characteristics, as predicted in simulations, hold true in practical implementations, reinforcing confidence in the design's effectiveness.

In the description of Fig. 7, it is mentioned that there is good agreement between the simulated and measured data; however, it is evident that noticeable differences exist between the simulation and measurement results. Discrepancies between simulated and measured values are common in antenna design due to several factors, such as fabrication tolerances, material inconsistencies, and environmental factors that are not fully captured in simulations. In this case, the claim of "good agreement" may be overstated, as the observed deviations indicate that the measured performance may not fully match the simulated predictions. Additionally, the descriptions for Figs. 7 and 8 appear to lack clarity and logical coherence. These figures should ideally present a consistent comparison, with a clear explanation of any deviations and a discussion on potential reasons for the observed discrepancies.

Figure 8 shows the simulated gain for the four switching states of the proposed antenna. The maximum gain 4.7 dBi is observed across the useful bandwidth. Fig. 7 illustrates the axial ratio plot for the proposed antenna, specifically focusing on its performance under different switching states where the

TABLE 3. Effect of slot dimensions on antenna performance.

Slot Width (mm)	Slot Depth (mm)	Resonant Frequency (GHz)	Bandwidth (MHz)	Impedance Matching (S_{11}, dB)	Gain (dBi)
1.0	0.5	10.1	620	-20	5.2
1.2	0.6	10.3	650	-22	5.5
1.5	0.7	10.5	700	-25	5.7
1.8	0.8	10.7	730	-18	5.3

diode configurations are toggled. In this context, the notation (0-Diode OFF and 1-Diode ON) indicates the specific states of the diodes that influence the antenna's polarization characteristics. The axial ratio is a key performance metric for antennas operating in circular polarization (CP), as it quantifies the symmetry of the electric field radiated by the antenna. A lower axial ratio, ideally below 3 dB, signifies effective circular polarization and minimal distortion in the transmitted signal.

In the presented axial ratio plot, the values consistently remain below the 3 dB threshold across the relevant frequency range, indicating that the antenna can effectively maintain circular polarization in its operational modes. This characteristic is crucial for applications such as satellite communication, where signal integrity and polarization matching are essential for optimal performance. The ability of the antenna to switch between left-hand circular polarization (LHCP) and right-hand circular polarization (RHCP) based on the diode states further enhances its versatility, allowing it to adapt to varying communication requirements.

Figure 8 complements this analysis by showcasing the simulated gain for the antenna across the four different switching states. The gain of an antenna is a critical parameter, as it reflects the ability of the antenna to focus energy in a particular direction, enhancing signal strength and improving overall communication efficiency. The maximum gain observed in this design is 4.7 dBi, achieved across the useful bandwidth of the antenna. This level of gain indicates a satisfactory performance level for many applications, particularly in the X-band frequency range where this antenna is intended to operate.

The consistency of the gain across the different switching states reinforces the design's effectiveness in maintaining high performance regardless of the operational mode. The achieved gain is significant for X-band applications, such as radar and satellite communications, where reliable signal transmission is paramount. Together, the results from Figs. 7 and 8 underscore the robustness of the proposed antenna design, demonstrating its capability to deliver high-quality circular polarization with effective gain across multiple configurations. This adaptability and performance reliability position the antenna as a suitable candidate for a range of advanced communication systems.

Where diode biasing condition is represented as 0-OFF & 1-ON.

The comparison in Table 2 between the simulated and measured results for the proposed antenna highlights the performance across various switch states, with close agreement between the two sets of data. The return loss (S_{11}) values indicate effective impedance matching, as seen from the similar values for both simulation and measurement, particularly in the switch state $St1 = 0$, $St2 = 0$, where the measured return loss is -14.1 dB compared to the simulated -14.7 dB. The -10 dB bandwidth percentage varies with the switch states, with the widest bandwidth of 8.4% in simulation and 8.1% in measurement observed for the left-hand circular polarization (LHCP) state $St1 = 0$, $St2 = 1$. The antenna achieves linear polarization (LP) in states where both diodes are OFF or ON and circular polarization (CP) when one diode is ON. The gain remains consistent across the switch states, with a maximum simulated gain of 4.7 dBi for the right-hand circular polarization (RHCP) state $St1 = 1$, $St2 = 0$, and a closely matching measured gain of 4.6 dBi. The axial ratio for CP is below 3 dB, with reflecting effective polarization, particularly in states with LHCP and RHCP, where the measured axial ratios are 1 dB and 1.2 dB, respectively. Fig. 9 shows the simulated radiation patterns of proposed antenna at four operating bands. The resonant frequencies are 10.2 GHz and 11.88 GHz for the linear polarization states. The maximum gains are found to be 2.4 dBi and 4.5 dBi, respectively. In these two frequencies, the cross polarization level is minimum. The proposed antenna has good linear polarization performance. The resonant frequencies are 11.06 GHz and 11.62 GHz for circular polarization states. The peak gains are found to be 4.1 dBi and 4.7 dBi, respectively. It is also noted that the discrepancy between the cross polarization and co-polarization is more than 10 dB over the main beam direction. The CP states have minimum axial ratio in the operating bands (AR $\leq$ 3 dB).

The findings across Tables 3 to 7 reveal how specific design modifications influence the performance of the miniature inverted V-slot reconfigurable patch antenna for X-band applications. Starting with slot dimensions, it is evident that as slot width and depth increase, there is a clear rise in the resonant frequency, which moves from 10.1 GHz with a 1.0 mm width to 10.7 GHz with a 1.8 mm width. Larger slots also broaden the bandwidth significantly, achieving a maximum of 730 MHz. However, while the impedance matching (S_{11}) initially improves with the slot size increase — indicating better signal reflection control — at the largest slot width, matching slightly decreases, suggesting a limit to the effectiveness of widening slots for impedance benefits. Additionally, the gain peaks at 5.7 dBi with a slot width of 1.5 mm, showing that oversized slots may compromise certain performance aspects like gain even while enhancing bandwidth. PIN diode positioning plays a critical role in frequency reconfiguration and polarization control. By adjusting the diode's position relative to the slot center and switching its bias condition, the

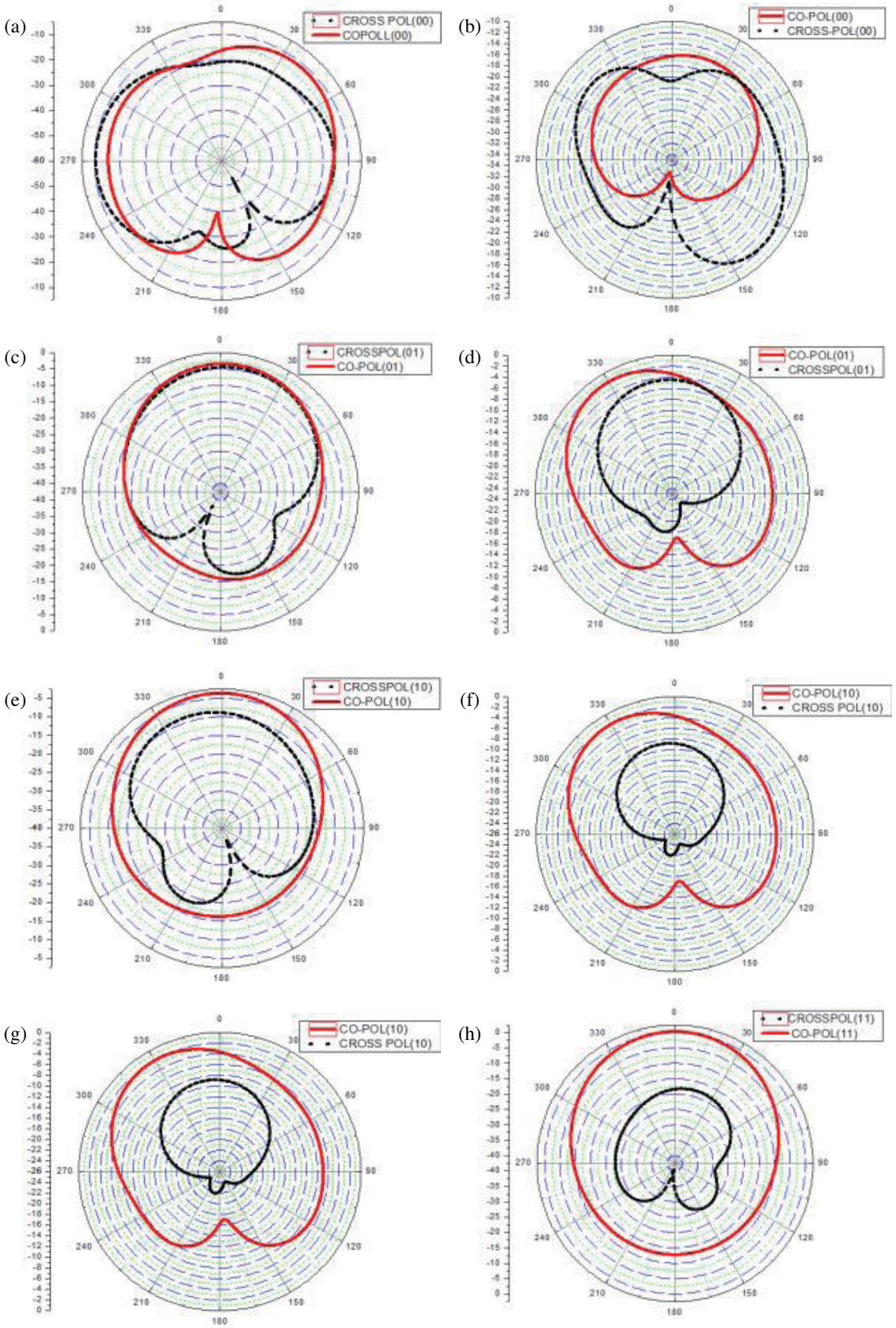

FIGURE 9. Simulated radiation pattern. (a) xz plane, $\Phi = 0^\circ$ (10.2 GHz). (b) xy plane, $\Phi = 90^\circ$ (10.2 GHz). (c) xz plane, $\Phi = 0^\circ$ (11.06 GHz). (d) xy plane, $\Phi = 90^\circ$ (11.06 GHz). (e) xz plane, $\Phi = 0^\circ$ (11.62 GHz). (f) xy plane, $\Phi = 90^\circ$ (11.62 GHz). (g) xz plane, $\Phi = 0^\circ$ (11.88 GHz). (h) xy plane, $\Phi = 90^\circ$ (11.88 GHz).

TABLE 4. Effect of PIN diode position on reconfiguration and polarization performance.

Diode Position (mm from Slot Center)	Bias Condition	Reconfigured Frequency (GHz)	Polarization	Return Loss (S_{11}, dB)	Switching Speed (ns)
0.5	Forward	9.9	RHCP	−21	35
0.7	Reverse	10.2	LHCP	−19	40
1.0	Forward	10.5	Linear	−23	30
1.2	Reverse	10.8	RHCP	−20	33

TABLE 5. Influence of defected ground structure (DGS) slot characteristics on gain and bandwidth.

DGS Slot Width (mm)	DGS Slot Depth (mm)	Frequency (GHz)	Bandwidth (MHz)	Gain (dBi)	Side Lobe Level (dB)
0.3	0.3	10.0	600	5.0	−15
0.5	0.5	10.2	650	5.4	−18
0.7	0.7	10.4	700	5.6	−20
0.9	0.9	10.6	740	5.3	−17

TABLE 6. Impact of patch size and corner modification on efficiency and polarization purity.

Patch Width (mm)	Patch Height (mm)	Frequency (GHz)	Efficiency (%)	Polarization Purity (%)	Gain (dBi)
10.0	13.5	10.2	85	90	5.1
10.5	14.0	10.4	87	92	5.4
11.0	14.5	10.6	89	94	5.6
11.5	15.0	10.8	90	91	5.3

TABLE 7. Thermal stability across different environmental conditions.

Temperature (°C)	Frequency (GHz)	Bandwidth (MHz)	Gain (dBi)	Impedance Matching (S_{11}, dB)
25	10.3	650	5.6	−22
50	10.2	640	5.5	−21
75	10.1	630	5.3	−20
100	10.0	620	5.0	−18

antenna can shift between different polarization modes, such as RHCP, LHCP, and LP. For instance, when the diode is placed 0.5 mm from the slot center and in forward bias, the frequency is set at 9.9 GHz with RHCP, achieving fast switching speed at 35 ns. Further from the slot center, frequencies shift upwards, reaching 10.8 GHz with RHCP when the diode is 1.2 mm away. The return loss (S_{11}) remains stable, showing effective impedance matching across these configurations, which is crucial for adaptable, multi-functional antenna use.

The Defected Ground Structure (DGS), which incorporates slots of varying width and depth, influences the antenna's frequency and side lobe suppression capabilities. With increasing DGS slot size, both frequency and bandwidth expand, as shown by the 10.6 GHz frequency and 740 MHz bandwidth at the largest slot dimensions. The gain remains relatively steady, peaking at 5.6 dBi, but slightly declines with the largest DGS slots. Importantly, side lobe levels improve with moderate slot sizes, indicating a well-managed radiation pattern without excessive unwanted radiation, which is advantageous in applications requiring directional focus. The patch size and corner modifications add another layer of performance enhancement. As the patch size grows from 10.0 mm × 13.5 mm to 11.5 mm × 15.0 mm, the antenna's efficiency improves, peaking at 90%, and polarization purity reaches 94% at 11.0 mm × 14.5 mm. This balance suggests an optimal patch size for achieving high purity and efficiency, as further increases do not proportionally improve performance. This means that a compact design can be maintained while still achieving high efficiency and purity, which is essential for space-constrained applications. Lastly, thermal stability testing under temperatures from 25°C to 100°C shows that while there is a slight reduction in bandwidth (from 650 MHz to 620 MHz) and gain (from 5.6 dBi to 5.0 dBi) at higher temperatures, the impedance matching (S_{11}) remains relatively stable, only slightly increasing to −18 dB. This resilience indicates that the antenna can operate effectively across a range of temperatures, a critical feature for real-world applications where environmental factors vary.

The proposed microstrip antenna has the following features.

TABLE 8. Comparison of the proposed work with the existing art of work.

Reference	Antenna Size (mm^2)	Reconfiguration Type	Activators	BW (MHz)	Gain (dBi)	Polarization
[7]	56.8×4	Polarization	4 PIN Diodes	34/56/53	NR	LP/LHCP/RHCP
[8]	232.2×232.2	Polarization	2 PIN Diodes	30	3.7/4.6	LP/C
[10]	21×9	Frequenc	5 PIN Diodes	1300/3500/3300	1.9/2.8/4	LP
[11]	18.5×7	Polarization	4 PIN Diodes	23	1.	LP/LHCP/RHCP
[12]	32×3	Frequenc	6 PIN Diodes	2000/2170/2190	3.4/4/4.2	LP
[14]	60×6	Frequency and polarization	4 PIN Diodes	NR	4.5/3.89	LP/C
[15]	50×4	Frequency and polarization	2 PIN Diodes	14	3/3.2	LP/C
[20]	50×40	Frequency	3 PIN Diodes	1500/2500/3000	3.0/4.5/4.8	LP
[21]	60×60	Frequency and polarization	4 PIN Diodes	200/300/450	2.5/3.5/4.0	LP/CP
[22]	70×50	Polarization	2 PIN Diodes	500	3.5	LHCP/RHCP
Proposed Work	27×25	Frequency and polarization	2 PIN Diodes	620/930/900/500	2.4/4.1/4.7/4.5	LP/LHCP/RHCP

(i) This antenna is used for both frequency and polarization reconfiguration.

(ii) It is a very small antenna compared to [7, 8, 11, 12, 14, 15].

(iii) Bandwidth offered by this antenna is very high compared to [7, 8, 11, 14, 15].

(iv) Number of activators is smaller than [7, 10–14].

(v) The proposed antenna operates at four bands but the antennas [7–15], and all antennas operating bands are less than four.

The return loss measurement of fabricated antenna using network analyzer is shows in Fig. 10.

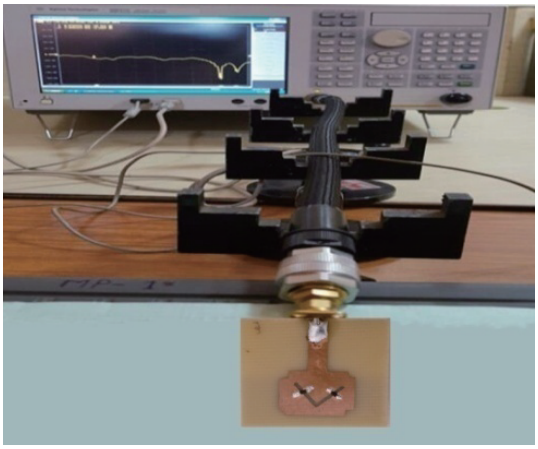

FIGURE 10. Fabricated antenna testing on network analyzer.

Comparison of the proposed work with the existing art is presented in Table 8. The proposed design has small size compared to all antennas mentioned in Table 8.

Figure 9 illustrates the simulated radiation patterns of the proposed microstrip antenna at various frequencies and planes. The patterns are depicted for both the xz plane ($\Phi = 0°$) and xy plane ($\Phi = 90°$) at frequencies of 10.2 GHz, 11.06 GHz, 11.62 GHz, and 11.88 GHz. These patterns demonstrate the antenna's performance in terms of its directional radiation characteristics across different operational frequencies, highlighting its potential for both frequency and polarization reconfiguration.

The proposed antenna exhibits several noteworthy features that set it apart from other designs. Firstly, it facilitates frequency and polarization reconfiguration, making it versatile for various applications. Secondly, its compact size (27 mm × 25 mm) is significantly smaller than the antennas referenced in previous studies [7, 8, 11, 12, 14, 15]. Moreover, the bandwidth of the proposed antenna is higher than the antennas listed, allowing for greater operational flexibility. Additionally, it requires fewer actuators than the other designs, with only two PIN diodes compared to the higher number found in the referenced works. Importantly, the proposed antenna operates effectively across four distinct frequency bands, whereas the antennas in [7–15] operate on fewer than four bands, enhancing its utility in diverse applications. The activators for the proposed design include only 2 PIN diodes, which is fewer than other designs with similar functionalities, like [10] (5 PIN diodes) and [12] (6 PIN diodes). This lower number of diodes helps reduce complexity and power consumption. The bandwidth (BW) of the proposed antenna spans multiple frequencies (620, 930, 900, and 500 MHz), allowing for versatile usage across a wide range of frequencies.

The proposed design also achieves competitive gain values of 2.4, 4.1, 4.7, and 4.5 dBi across different frequencies, offering stable performance. For polarization, the antenna supports linear polarization (LP), left-hand circular polarization (LHCP), and right-hand circular polarization (RHCP), making it adaptable for various signal requirements. In comparison,

other designs provide limited polarization options, with only a few offering LHCP/RHCP flexibility (e.g., [7] and [22]).

Figure 10 showcases the return loss measurements of the fabricated antenna, obtained using a network analyzer, further validating the design's effectiveness. Additionally, Table 8 provides a comparative analysis between the proposed work and existing antenna designs. The table highlights the advantages of the proposed design, emphasizing its compact size, minimal activators, and substantial bandwidth, while also showcasing its gain and polarization capabilities. This comparison underscores the proposed antenna's superior performance characteristics, reinforcing its potential for application in advanced communication systems.

4. CONCLUSION

The proposed reconfigurable patch antenna for X-band applications demonstrates significant advancements in both frequency and polarization reconfiguration, offering a versatile solution for modern communication systems. With its compact design, measuring only 27 mm × 25 mm, the antenna achieves remarkable performance across four operational frequency bands (9.84–10.20 GHz, 10.66–11.59 GHz, 11.08–11.98 GHz, and 11.61–12.11 GHz). Incorporating two PIN diodes facilitates efficient switching between states, resulting in improved bandwidth and gain characteristics, particularly for circular polarization. Notably, the antenna's bandwidth and minimal number of activators surpass those of existing designs, providing a competitive edge in terms of efficiency and adaptability. The measured results, including low VSWR and favorable axial ratio, confirm the antenna's reliable performance, making it an excellent candidate for applications requiring dynamic reconfiguration capabilities. The design of a novel miniature inverted 'V' slot microstrip patch antenna with reconfigurable frequency and polarization effectiveness has been conferred in this article. The frequency reconfiguration and LHCP and RHCP polarization reconfigurations are achieved by controlling the PIN diodes. All of the experimental and simulated results conferred very well with the proposed antenna used for X-band military applications.

ACKNOWLEDGEMENT

The authors wish to acknowledge the Lotus Antenna Testing Company, Hyderabad, providing testing facility. We would like to thank K. Sambasiva Rao, DRDO (RCI Lab) scientist, Hyderabad for his helpful suggestions. We are also thankful to MVGR College of Engineering, Vizianagaram providing requirements in completion of this paper.

REFERENCES

[1] Ismail, M. F., M. K. A. Rahim, M. R. Hamid, H. A. Majid, A. H. Omar, L. O. Nur, and B. S. Nugroho, "Dual-band pattern reconfigurable antenna using electromagnetic band-gap structure," *AEU — International Journal of Electronics and Communications*, Vol. 130, 153571, 2021.

[2] Ebrahimi, E., J. R. Kelly, and P. S. Hall, "Integrated wide-narrowband antenna for multi-standard radio," *IEEE Transactions on Antennas and Propagation*, Vol. 59, No. 7, 2628–2635, 2011.

[3] Tawk, Y., J. Costantine, K. Avery, and C. G. Christodoulou, "Implementation of a cognitive radio front-end using rotatable controlled reconfigurable antennas," *IEEE Transactions on Antennas and Propagation*, Vol. 59, No. 5, 1773–1778, 2011.

[4] Chandra, K. V., M. Satyanarayana, and K. T. Battula, "A novel miniature hexagonal shape switched pattern and frequency reconfigurable antenna," *International Journal of Communication Systems*, Vol. 33, No. 5, e4264, 2020.

[5] Bkassiny, M., S. K. Jayaweera, and K. A. Avery, "Distributed Reinforcement Learning based MAC protocols for autonomous cognitive secondary users," in *2011 20th Annual Wireless and Optical Communications Conference (WOCC)*, 1–6, Newark, NJ, USA, 2011.

[6] López-Marcos, F., R. Torrealba-Meléndez, and E. I. Tamariz-Flores, "Analysis and design of a reconfigurable antenna for ISM and GSM bands for cognitive radio applications," in *2015 International Conference on Electronics, Communications and Computers (CONIELECOMP)*, 66–71, Cholula, Mexico, Feb. 2015.

[7] Parihar, M. S., A. Basu, and S. K. Koul, "Polarization reconfigurable microstrip antenna," in *2009 Asia Pacific Microwave Conference*, 1918–1921, Singapore, Dec. 2009.

[8] Sung, Y. J., "Reconfigurable patch antenna for polarization diversity," *IEEE Transactions on Antennas and Propagation*, Vol. 56, No. 9, 3053–3054, 2008.

[9] Michel, A., M. R. Pino, and P. Nepa, "Reconfigurable modular antenna for NF UHF RFID smart point readers," *IEEE Transactions on Antennas and Propagation*, Vol. 65, No. 2, 498–506, 2017.

[10] Srivastava, G., A. Mohan, and A. Chakrabarty, "Compact reconfigurable UWB slot antenna for cognitive radio applications," *IEEE Antennas and Wireless Propagation Letters*, Vol. 16, 1139–1142, 2016.

[11] Wu, F. and K. M. Luk, "A compact and reconfigurable circularly polarized complementary antenna," *IEEE Antennas and Wireless Propagation Letters*, Vol. 16, 1188–1191, 2016.

[12] Gholamrezaei, M., F. Geran, and R. A. Sadeghzadeh, "Completely independent multi-ultrawideband and multi-dual-band frequency reconfigurable annular sector slot antenna (FR-ASSA)," *IEEE Transactions on Antennas and Propagation*, Vol. 65, No. 2, 893–898, 2017.

[13] Chandra, K. V., M. Sathyanarayana, and B. T. Krishna, "Design of polarization and frequency reconfigurable rectangular patch antenna for cognitive radio applications," *JARDCS*, Vol. 11, No. 01, 2019.

[14] Vijaya Chandra, K., M. Sathyanarayana, and B. T. Krishna, "A novel polarization and frequency reconfigurable antenna for cognitive radio applications," *JWE*, Vol. 18, No. 4, 5084–5088, 2019.

[15] Tawk, Y., J. Costantine, and C. G. Christodoulou, "Cognitive-radio and antenna functionalities: A tutorial," *IEEE Antennas and Propagation Magazine*, Vol. 56, No. 1, 231–243, 2014.

[16] Grau, A., J. Romeu, M.-J. Lee, S. Blanch, L. Jofre, and F. D. Flaviis, "A dual-linearly-polarized MEMS-reconfigurable antenna for narrowband MIMO communication systems," *IEEE Transactions on Antennas and Propagation*, Vol. 58, No. 1, 4–17, 2010.

[17] Jin, Z.-J., J.-H. Lim, and T.-Y. Yun, "Frequency reconfigurable multiple-input multiple-output antenna with high isolation," *IET Microwaves, Antennas & Propagation*, Vol. 6, No. 10, 1095–1101, 2012.

[18] Mahmood, S. M. and T. A. Denidni, "Pattern-reconfigurable antenna using a switchable frequency selective surface with improved bandwidth," *IEEE Antennas and Wireless Propagation Letters*, Vol. 15, 1148–1151, 2015.

[19] Nguyen-Trong, N., L. Hall, and C. Fumeaux, "A frequency-and pattern-reconfigurable center-shorted microstrip antenna," *IEEE Antennas and Wireless Propagation Letters*, Vol. 15, 1955–1958, 2016.

[20] Abdollahvand, M., Y. Zehforoosh, B. Marufi, P. E. Kaleybar, and A. Dastranj, "A novel UWB in-body printed microstrip feed monopole antenna with dual band-stop capabilities," *Microwave and Optical Technology Letters*, Vol. 66, No. 9, e34317, 2024.

[21] Abdollahvand, M., B. A. Arand, K. Katoch, and S. Ghosh, "A novel and compact ultra-wideband printed monopole antenna with enhanced bandwidth and dual-band stop properties," *Microwave and Optical Technology Letters*, Vol. 66, No. 1, e33990, 2024.

[22] Çelik, K., "A novel circular fractal ring UWB monopole antenna with dual band-notched characteristics," *ETRI Journal*, Vol. 46, No. 2, 218–226, 2024.

[23] Benkhadda, O., M. Saih, A. Reha, S. Ahmad, K. Chaji, H. Singh, and A. J. A. Al-Gburi, "A miniaturized reconfigurable antenna for modern wireless applications with broadband and multi-band capabilities," *Progress In Electromagnetics Research M*, Vol. 127, 93–101, 2024.